A Letters Journal Exploring the Frontiers of Physics

August 2007

EPL, **79** (2007) 34001
doi: 10.1209/0295-5075/79/34001

www.epljournal.org

A mean-field model for the rheology and the dynamical phase transitions in the flow of granular matter

B. Andreotti

Laboratoire de Physique et Mécanique des Milieux Hétérogènes, UMR 7636 CNRS, Université Paris 7 10 rue Vauquelin, 75231 Paris Cedex 05, France

received 8 November 2006; accepted in final form 14 June 2007
published online 13 July 2007

PACS 45.70.Mg – Granular flow: mixing, segregation and stratification
PACS 83.50.Ax – Steady shear flows, viscometric flow

Abstract – Based on a large set of experiments and numerical simulations, it has been recently shown (GDR MiDi (collective work), *Eur. Phys. J. E*, **14** (2004) 341) that dense granular flows are well described by a local rheology: the ratio of the shear stress τ to the normal stress P is an increasing function of the properly rescaled shear rate I. We propose a mean field model for this quasi-local constitutive relation and the phase diagram of granular matter, based on the motion of single spherical grain on an array of identical grains. The model recovers a "solid-liquid" transition that is controlled by potential trapping, as well as a subcritical "liquid-gas" transition governed by the restitution coefficient. The system presents a "triple point" above which the grain directly leaves the static equilibrium to enter the gaseous regime. In the liquid regime, the relation between force and velocity is found to be almost independent of the microscopic parameters, friction and restitution coefficient. The dynamics is dominated by potential trapping and leads to a constitutive relation of the form $\tau/P = \mu_d + \delta\mu \exp(-I_d/I)$, in close agreement with experimental and numerical results. This rheology is only quasi-local as the inertial number is redefined, introducing the effective number of grains $\mathcal{N}$ involved in a collision: $I = \dot{\gamma}\sqrt{\mathcal{N}m/Pd}$.

Granular matter can behave like a solid, a liquid or a gas. The basic problem is to derive the constitutive relations for each of the phases, starting from the dynamical mechanisms at the scale of the grain. In the last decade, there has been a strong effort to extend the methods developed in the 19^{th} century for continuous media to granular matter: anisotropic elasticity for the static equilibrium (solid phase), non-newtonian hydrodynamics for dense flows (liquid phase) and kinetic theory when the grains are strongly agitated (gaseous phase). In the present paper, we focus on the liquid phase, in particular on the transitions from solid to liquid and from liquid to gas. As shown in a recent collective paper [1], dense granular flows can be organized into two sub-classes. Under quasi-static flow conditions, the shear deformations can become strongly localized in organized regions of space (*e.g.* shear bands). In other situations, the shear is distributed over the whole flow range, and in this case the observed rheology is approximately governed by local laws [2]: the shear stress τ rescaled by the normal stress P is a function of the properly rescaled shear rate $\dot{\gamma}$:

$$\frac{\tau}{P} = \mu_I(I) \quad \text{with} \quad I = \frac{\dot{\gamma}}{\sqrt{Pd/m}}, \tag{1}$$

where m is the mass of the grains and d their diameter (see [3] for the extension to 3D). This constitutive relation can be interpreted either as a shear rate dependent friction or as a pressure-dependent viscosity. It is said to be *local* as the stress at a given place is a function of the shear rate at that place only. This property is directly related to the transmission of momentum among grains: the rheology is purely local, quasi-local or fully non-locally depending on whether the momentum lost by a grain in a collision is transmitted to the grain below it, to a small region of grains around it, or directly to the solid pile through a force chain [4]. Importantly, the generic prediction of kinetic theory is a *decrease* of μ_I with agitation (with I) [5]. On the contrary, measurements show an *increase* of μ_I with I, meaning that long-term contacts cannot be neglected in the "liquid" regime. As no collective effect is involved in a purely local rheology, we propose here an

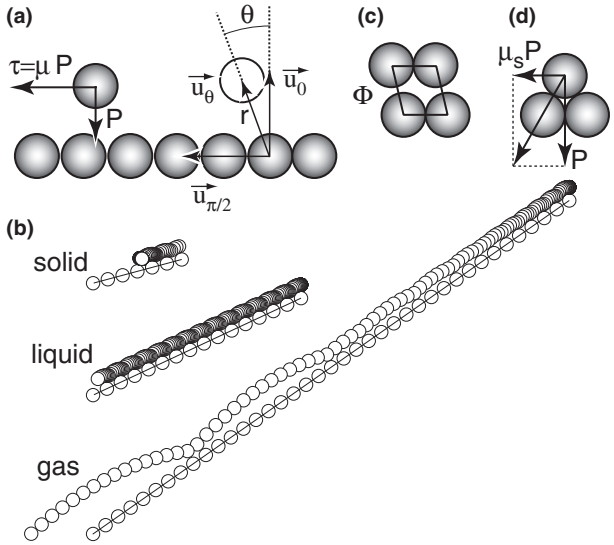

Fig. 1: (a) Schematic of the system. (b) Motion of a grain slightly pushed at initial time for $\mu = 0.15$ (top), $\mu = 0.4$ (middle) and $\mu = 0.7$ (bottom). (c) Schemtaic showing the relation between the packing fraction and the position: $\phi = \frac{\pi}{6r\cos\theta}$. (d) Schematic of the grain at the threshold shear stress $\mu = \mu_s = \tan(\pi/6)$.

analysis of momentum exchanges at the scale of a single grain and show that the correct shape of the law $\mu_I(I)$ can be recovered from a purely mechanical analysis. We then propose a discussion of non-local effects in extended granular flows.

Theoretical set-up. – The motion of a single grain on an inclined bumpy line has already been investigated in different contexts [6–9]. Here, we formulate the problem in a general framework, considering a single grain driven by a tangential force τd^2 and pushed back to contact by a normal force Pd^2 (fig. 1a). The situation of the inclined bumpy line (fig. 1b) is recovered as a particular case for which $P = mg\cos\alpha/d^2$ and $\tau = mg\sin\alpha/d^2$, where α is the inclination angle. For simplicity we do not investigate any dependence on the mean number of contacts. All the quantities are rescaled by P, m and d so that the system is controlled by a single non-dimensional parameter, the rescaled shear stress $\mu = \tau/P$. Depending on μ, three different regimes are observed (fig. 1b). At low shear stress ($\mu < \mu_d$), the grain always gets trapped in static equilibrium (solid phase). For $\mu_d < \mu < \mu_\infty$, the grain remains almost permanently in contact with the rough plane and makes periodic collisions dissipating the energy brought by the driving stress τ (liquid phase). At large shear stress ($\mu > \mu_\infty$), the particle motion accelerates and never reaches a steady state: the grain makes higher and higher bounces (gaseous phase). Even though this system is very simple, it thus presents the prominent features of certain granular systems [6,9].

The spherical grains that form the rough line are assumed to be in contact. The equations of motion are derived in polar coordinates (r, θ) centred on the closest grain (fig. 1). Introducing the unit vector $\vec{u}_\theta$ pointing along the direction θ, the grain position is $r\ \vec{u}_\theta$ and its instantaneous velocity is $\dot{r}\,\vec{u}_\theta + r\,\dot{\theta}\,\vec{u}_{\theta+\pi/2}$. Ω is the angular velocity of the grain around its diameter and j represents the moment of inertia (equal to 1/20 for the spherical grain considered here). The force at the contact point —when it exists— is decomposed into a radial component $N\vec{u}_\theta$ and a tangential component $T\vec{u}_{\theta+\pi/2}$, so that the equations of motion read

$$\begin{aligned} r\ddot{\theta} &= T - 2\dot{r}\dot{\theta} + \sin\theta + \mu\cos\theta, \\ \ddot{r} &= N + r\dot{\theta}^2 - \cos\theta + \mu\sin\theta, \\ \dot{\Omega} &= -T/(2j). \end{aligned} \tag{2}$$

The contact force is assumed to follow a Coulomb law of friction coefficient f: i) if the grain flies, $N = T = 0$; ii) if it rolls without sliding, $0 < |T| < fN$ and $\Omega = 2\dot{\theta}$; iii) if it slides, $|T| = fN$ and T opposes the sliding velocity $(\dot{\theta} - \Omega/2)$. Rolling friction is assumed to be negligible, compared to the effect of collisions. We assume that the collisions ($r = 1$ and $\dot{r} < 0$) are inelastic and take a time δt negligible compared to the time between collisions. Introducing the restitution coefficient e, the normal velocity $\dot{r}^+$ after the collision is equal to $-e\dot{r}^-$. The superscript $(+)$ and $(-)$ refer to the quantity after and before the collision respectively. The normal force is thus given by $N\delta t = \dot{r}^+ - \dot{r}^- = -(1+e)\dot{r}^-$ and the change of the angular velocities by $\dot{\theta}^+ = \dot{\theta}^- + T\delta t$ and $\Omega^+ = \Omega^- - T\delta t/2j$. We assume that the same friction law can be applied during the collision, *i.e.* that $|T\delta t| = \max(fN\delta t, |\dot{\theta}^- - \Omega^-/2|)$. Note that we only treat binary collisions: if the grain is rolling on another grain when the collision occurs, only the collided grain is assumed to exert diverging forces.

Phase diagram. – For given microscopic parameters (e and f), we characterize the state of the system by the rescaled shear stress μ, by the packing fraction Φ (fig. 1c) and by a coarse grained velocity $v(t)$, defined as the inverse of the time $\tau(t)$ needed to make a displacement by d: $[r\sin\theta]_{t-\tau/2}^{t+\tau/2} = 1$. The phase diagram is shown on fig. 2 for the reference case: $e = 0$ and $f = 0$. By definition, the solid state ① is along the line $v = 0$: the grain can remain trapped between neighbouring grains below it for $\mu < \mu_s$ (fig. 1c) while above μ_s, it spontaneously starts rolling. If the grain initially at rest is pushed with sufficient energy to escape from potential trapping, its velocity increases and quickly saturates to an asymptotic value (liquid branch ③). The solid and liquid states are thus separated by the unstable branch ② for which the grain is also static, but right on top of the grain underneath it (at $\tan\theta = -\mu$). As v is still null, the unstable branch collapses on the stable one in the (v, μ) plane, but they differ by the packing fraction Φ (fig. 2b).

The cut-off of the liquid branch ③ at the dynamical friction coefficient μ_d directly originates in the fact that

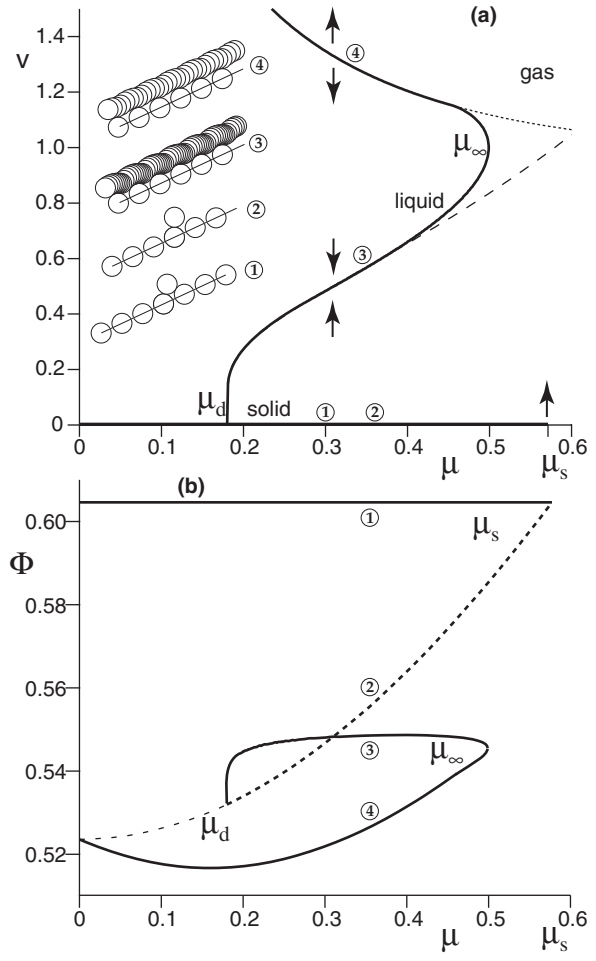

Fig. 2: (a) Phase diagram in the (v, μ)-plane, for $e = 0$ and $f = 0$. The branches separating the different states correspond to macroscopic steady states *i.e.* to periodic solutions of eq. (2): ① the grain is at rest between neighbouring grains below it. ② the grain is on top of the grain underneath. ③ the grain is rolling down the line. ④ the grain flies from bump to bump and takes off immediately after each collision. The unstable branch ② separates the solid from the liquid state and the unstable branch ④ the liquid from the gaseous state. The dashed and dotted lines corresponds to the analytical approximations of the branches ③ (eq. (3)) and ④ (eq. (4)) (b) Phase diagram in the (Φ, μ)-plane.

the grain has to jump energy gaps (associated to the pressure P) to move along the line. Close to a maximum of potential energy, the mechanical energy can be generically written under the non-dimensional form $E = \dot{x}^2 - x^2$, where x is the coordinate. So the time needed to get over it and cover a unit distance is

$$\tau = \int \frac{\mathrm{d}x}{|\dot{x}|} = \int \frac{\mathrm{d}x}{\sqrt{E + x^2}} = \left[\sinh^{-1}(x/\sqrt{E})\right] \sim -\frac{1}{2}\ln E.$$

The energy is governed by the equilibrium between the driving force (proportional to μ) and the dissipation induced by collisions (proportional to the kinetic energy). It follows that the kinetic energy just after a collision is proportional to μ. At the threshold $\mu = \mu_d$, this kinetic energy is just sufficient to escape from the potential trap ($E = 0$). So the mechanical energy E is proportional to $\mu - \mu_d$. Close to the threshold, v thus behaves as

$$v = \frac{1}{\tau} = \frac{I_d}{\ln\left(\frac{\delta\mu}{\mu - \mu_d}\right)}. \tag{3}$$

Figure 2 (dashed line) shows that this asymptotic behaviour remains close to the exact relation, determined numerically, in almost the whole liquid regime. This unusual logarithmic bifurcation comes from the localisation of energy dissipation during collisions. An overdamped dynamics, like that observed when grains are flowing in a viscous liquid, leads instead to a standard saddle node bifurcation ($v \propto \sqrt{\mu - \mu_d}$). Figure 3a-c shows the dependence of the parameters I_d and μ_d with e and f. The liquid branch ③ turns out to be almost independent of e and f. This essentially means that the dissipation of the radial kinetic energy after a collision takes place during a time small compared to the period τ. In other words, the collision is effectively fully inelastic, even for a non-zero restitution coefficient e. The macroscopic friction μ_d very slightly decreases when the microscopic friction f increases from 10^{-2} to 10^{-1} (fig. 3a). This surprising behaviour comes from the absence of rotation at low friction, which reduces the restitution of energy during collisions. As a conclusion, the solid-liquid transition essentially depends on geometrical effects, namely on μ_s.

Above the third friction coefficient μ_∞, the grain no longer reaches a steady state: it takes off the bumpy line and bounces higher and higher, making less and less collisions and thus dissipating less and less energy. As shown on fig. 3b, the liquid-gas transition is controlled by the restitution coefficient e. The maximum friction coefficient μ_∞ decreases with e up to $\simeq 0.75$, at which the domain of existence of the liquid state disappears. Above this "triple point", the grain directly goes from the static to the accelerated regime. Surprisingly, this liquid-gas transition is subcritical: if sufficient energy is initially given, the grain motion can also become accelerated below μ_∞. The liquid and gaseous states are thus separated by an unstable branch ④ that corresponds to the periodic motion of a grain bouncing from bump to bump. Solving the energy balance between driving and dissipation under the requirement that the trajectory is composed by a succession of identical parabolic flights of unit length, we get the macroscopic velocity

$$v = \sqrt{\frac{(1+\mu^2)(1-e)}{2(\mu - f)(1+e)}} \tag{4}$$

shown on fig. 2 (dotted line).

Constitutive relation. – We define the effective friction μ_I exerted on the grain by the neighbouring grains

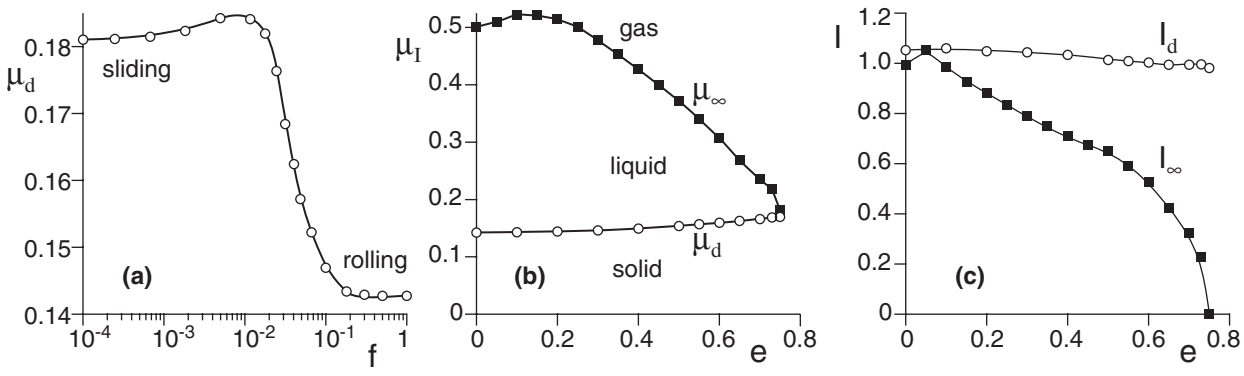

Fig. 3: Dependence of the solid-liquid ($\circ$ μ_d) and liquid-gas ($\blacksquare$ μ_∞) transition points as a function (a) of the contact friction f (for $e=0$) and (b) of the restitution coefficient e (for $f=0.25$). (c) Dependence of I_d and I_∞ on the restitution coefficient e.

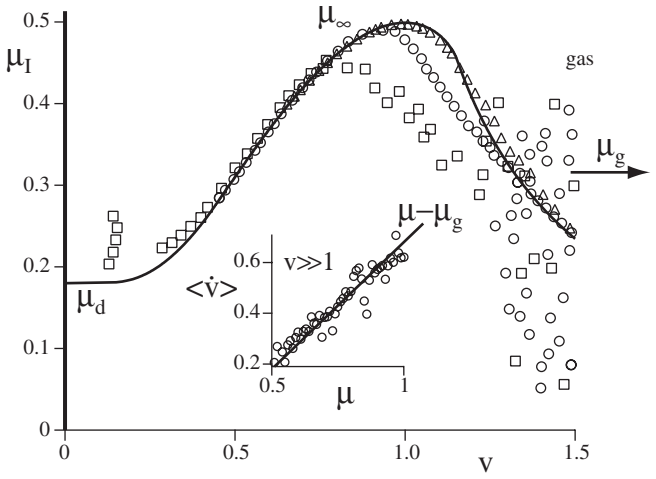

Fig. 4: (a) Friction $\mu_I = \mu - \dot{v}$ as a function of the rescaled velocity v. The solid line is derived from the periodic solutions shown in fig. 2. The symbols are measurements during transient motion for $\mu=0.15$ ($\square$), $\mu=0.30$ ($\circ$) and $\mu=0.45$ ($\triangle$). (b) Ensemble average of the grain acceleration in the gaseous regime as a function of μ ($\circ$). The solid line corresponds to the best fit by eq. (5), with a constant μ_I equal to $\mu_g \simeq 0.32$.

below it from the macroscopic momentum equation:

$$\dot{v} = \mu - \mu_I. \tag{5}$$

An important question is to determine whether the grain velocity v is sufficient to characterise μ_I. Assuming that it is indeed the case, $\mu_I(v)$ can be determined from the steady-state solutions ($\dot{v}=0$) shown on fig. 2. For each value of μ, we get the value of v for which $\mu_I(v)=\mu$ (solid line on fig. 4). Alternatively, μ_I can be determined by measuring both the acceleration $\dot{v}$ and the velocity v during the transients. The symbols on fig. 4 show the different measurements of $\mu_I = \mu - \dot{v}$ as a function of v extracted from the numerical integration of (2). The different measurements collapse on a single curve in the dense liquid regime, for moderate v, which means that the velocity v is sufficient to describe the "macroscopic" state of the system. Inverting eq. (3), we find the generic behaviour in the liquid state $\mu_I(v) = \mu_d + \delta\mu \exp(-I_d/v)$. This ceases to be valid when approaching to the maximum stable velocity I_∞, *i.e.* close to the liquid-gas transition.

While the positions at which collisions occur are deterministic at small v, they become random when the grain makes large hops *i.e.* they no more depend only on the grain velocity. As the impact angle controls the loss of momentum in collisions, the measurements of μ_I are scattered in the gaseous regime (fig. 4). As a consequence, we have performed an ensemble averaging over initial conditions to measure the effective friction. Figure 4b shows that μ_I tends toward a constant independent of v and μ in the accelerated regime ($1 \ll v$). Things get more complicated around the liquid-gas transition ($v \simeq 1$) as the grain trajectory is neither completely determined by v nor completely chaotic: μ_I both depends on μ and v (symbols on fig. 4). To summarize, a friction law $\mu_I(v)$ is recovered in the whole liquid regime, but also in the transition zone if μ is sufficiently close to μ_∞. In the gaseous regime, μ_I tends toward a constant μ_g smaller than μ_∞. This results from a loss of momentum per collision proportional to $\dot{\gamma}$ and a collision rate decreasing as $Pd/m\dot{\gamma}$.

From a single grain to an avalanche. – Our aim is now to use these results to provide an interpretation of observations and measurements performed in extended granular flows. Let us first assume that the rheology is local. This means i) that the velocity fluctuations induced by the potential wells are not correlated in space, and ii) that the momentum is exchanged through first neighbors. Expressing the relative velocity between grains in contact as $v \simeq \dot{\gamma} d$, we predict a constitutive relation of the form

$$\mu_I = \mu_d + \delta\mu \, \exp(-I_d/I). \tag{6}$$

Figure 5 shows that this prediction agrees remarkably well with existing measurements [1], both in the inclined plane [10] and in the plane shear [2] configurations. In particular, the present model predicts an increase of μ_I

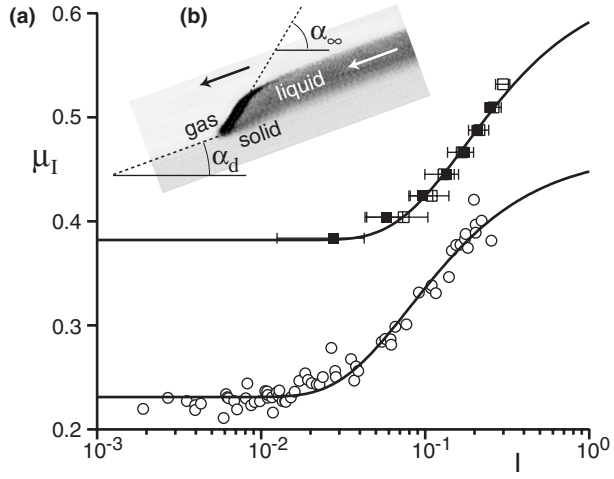

Fig. 5: (a) Comparison of the effective friction μ_I as a function of I in the plane shear (2D numerical simulation ○) and the inclined plane (experiment in 3D with 500 μm glass beads on a rough plane made of 500 μm (■) and 1300 μm (□) beads), after [1] fig. 8. The solid lines are the best fits by eq. (6). (b) Avalanche front visualized in a channel experiment, 30 mm in width ($d = 250\,\mu$m). The flowing layer appears in black and the static pile in gray. The transverse scale is 4 times the longitudinal one. Just at the wetting front, we predict a selection of the solid-liquid interface slope to $\mu_d = \tan\alpha_d$ and of the free surface slope to $\mu_\infty = \tan\alpha_\infty$.

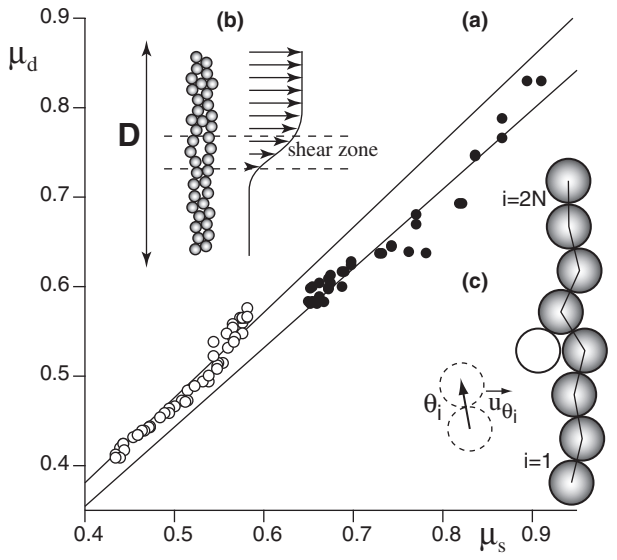

Fig. 6: Non-local effects. (a) Dynamical friction $\mu_d(h)$ as a function of the static friction $\mu_s(h)$ for a granular layer of thickness h on an inclined plane; (○) 500 μm glass beads on a rough plane made of the same beads; (●) 300 μm Fontainebleau sand on velvet. (b) Schematic of a shear band below a plug flow. (c) Schematic of a granular chain during a collision.

with I while kinetic theory predicts a decrease of friction with agitation. This is simply due to the different roles played by velocity fluctuations in the liquid and gaseous regime. At low I, the fluctuations are slaved to the average motion through the potential landscape: as the collision rate increases as $\dot\gamma$, the effective friction μ_I increases with I. At high I, the kinetic theory becomes valid and μ_I decreases with I. Interestingly, these arguments can be extended to other out-of-equilibrium systems, for instance a Lennard-Jones fluid at zero temperature. In that case, the potential trapping is not only induced by the external pressure but also by cohesion.

In the single grain model, the solid-liquid and liquid-gas phase transitions are controlled by the tangential-to-normal stress ratio μ and both transitions are hysteretic. The solid-liquid transition mainly depends on geometrical effects —encoded here into μ_s— with sub-dominant dependence on f and e. The liquid-gas transition, on the other hand, mostly depends on the restitution coefficient e. Both transitions are observed in spatially extended systems like the inclined plane geometry. In particular, the subcritical feature of the liquid-gas transition has been demonstrated experimentally at moderate angles but large injection velocity [11]. By definition, avalanche fronts are places at which phase transitions occur. During its formation, a wetting front such as shown on figure 5 tends to steepen, as the grains velocity increases with height ($\dot\gamma > 0$). When the front slope reaches μ_∞, the surface grains get ejected and form a small gaseous layer down-slope the front. We thus predict the selection of the avalanche front slope with respect to horizontal to be μ_∞, while the slope of the solid liquid interface reaches μ_d. The experimental measurements performed in the inclined plane geometry [10] are clearly consistent with this prediction. This selection of contact angle is reminiscent of the wetting of a substrate by a liquid. It pushes further the close analogy between the cohesion of condensed matter and the inelasticity of dry granular matter, yet non-cohesive.

Non-local effects. – Three observations evidence the existence of non-local effects in granular flows [1,12]. i) The dynamical friction depends on the granular layer thickness in the inclined plane geometry. The only interpretation given so far relates this effect to the diffusion of granular temperature, in the framework of kinetic theory [4]. However, the static friction μ_s —the slope at which motion starts— depends on the thickness *in the same way.* The mechanical model presented here suggests another interpretation based on potential trapping. As in the single grain problem, a grain in the bulk of a flow has to overcome energy barriers but the potential landscape in which it moves can be slightly different from that imposed at the boundary. As μ_s precisely characterizes the energy gap, the model predicts that μ_d should be proportional to μ_s [9]. Experimental data reasonably follows this relation (fig. 6), both for glass beads and for sand. This non-local effect can be integrated into eq. (6) through a dependence of the parameter μ_s with the distance to the boundary. ii) It has been observed experimentally and numerically

that the shear rate $\dot{\gamma}$ does not vanish at the free surface of gravity-driven flows while the shear stress should, in standard continuum mechanics. As mentioned earlier, the grains flowing at the surface are submitted to their own weight, *i.e.* to a trapping potential $P = \rho g d$. This simply means that the standard hydrostatic pressure $P = \rho g(h - z)\cos\alpha$ needs to be replaced by $P = \rho g(h - z + d)\cos\alpha$, when using a continuum description. iii) At small I, one often observes the formation of shear bands that cannot be explained by a local rheology. Shear localisation is often observed in confined geometries [1]. Having in mind the dynamical mechanisms discussed here, this observation can receive a simple interpretation. Consider for instance the shear cell sketched on fig. 6b, in which a velocity difference is imposed at two plates distant from D. Due to the grains elasticity, the confinement induces an extra-stress that adds to the mean pressure P, making the potential wells deeper. If a linear velocity profile is selected, all grains move with respect to the others, leading to a typical grain deformation proportional to d. If the shear localizes over few grain diameters, the grain deformation is proportional to d^2/D. If the confinement-induced stress is comparable to P, the energy gap may be smaller if the shear localises. As a conclusion, the rheology can become non-local as soon as the pressure —and thus the trapping potential— is not imposed.

Can we predict the strain-stress relation in the shear zone? Let us consider the simple situation described in fig. 6c in which momentum is exchanged along a single granular chain of length $2\mathcal{N}$ during collisions. $\mathcal{N}$ can be thought of as the length over which the direction of contact θ_i between the grains labelled i and $i+1$ decorrelates. The kinetic energy T of the system in the centre-of-mass reference frame is $T = \alpha_{i,j}\cos(\theta_i - \theta_j)\dot{\theta}_i\dot{\theta}_j$, with $\alpha_{i,j} = \min(i,j) - ij/2\mathcal{N}$. Then consider that the grain labelled $\mathcal{N}+1$, which was previously rolling on the grain shown in white in fig. 6c, collides with grain $\mathcal{N}$. One easily shows [5] that the exchange of momentum during the collision is governed by

$$\sum_{i=1}^{2\mathcal{N}-1} \alpha_{in}\cos(\theta_i - \theta_n)(\dot{\theta}_i^+ - \dot{\theta}_i^-) = -\frac{2\alpha_{\mathcal{N}n}\mu_s}{\sqrt{1+\mu_s^2}}\sin(\theta_n)\dot{\theta}_{\mathcal{N}}^-,$$

where $\dot{\theta}_i^-$ and $\dot{\theta}_i^+$ are the angular velocities just before and after the collision, respectively. Assuming that the angles θ_i are randomly distributed in some narrow interval around 0, except the angle between colliding grains $\theta_{\mathcal{N}} = \tan^{-1}(\mu_s)$, the previous equation gives, once averaged over the possible configurations: $\sum_i \alpha_{in} < (\dot{\theta}_i^+ - \dot{\theta}_i^-) > \propto -\alpha_{\mathcal{N}\mathcal{N}}\dot{\theta}_{\mathcal{N}}^-$. The contribution to the shear stress τ_i of the collisions between the grains $\mathcal{N}$ and $\mathcal{N}+1$ is the collision rate $\simeq \dot{\gamma}_{\mathcal{N}}$ times the momentum flux during one collision: $2\tau_i - \tau_{i+1} - \tau_{i-1} \propto \sum_{\mathcal{N}} \left[\dot{\gamma}\,(\dot{\theta}_i^+ - \dot{\theta}_i^-)\right]_{\mathcal{N}}$. Inverting the relation, we get that the contribution of collisions to the shear stress, $\mathcal{N}\dot{\gamma}_{\mathcal{N}}\dot{\theta}_{\mathcal{N}}^-$, is $\mathcal{N}$ times larger than for a single grain. This result can be inferred in a less formal way: if $\mathcal{N}$ grains are moving coherently the exchange of momentum during a collision is equivalent to that of a single grain having an effective mass $\mathcal{N}m$.

Interestingly, if θ_i becomes correlated over the whole pile (which is possibly the case close to the jamming transition), $\mathcal{N}$ becomes determined by the distance to the free surface: as shown in [5], an almost linear velocity profile is then observed. This is precisely the behavior obtained in numerical simulations [1].

* * *

I thank J. Snoeijer, O. Pouliquen and P. Claudin for their critical reading of the manuscript. This study was supported by an ACI Jeunes Chercheurs.

REFERENCES

[1] GDR MiDi (collective work), *Eur. Phys. J. E*, **14** (2004) 341.
[2] da Cruz F., Emam S., Prochnow M., Roux J.-N. and Chevoir F., *Phys. Rev. E*, **72** (2005) 21309.
[3] Jop P., Forterre Y. and Pouliquen O., *Nature*, **441** (2006) 727.
[4] Pouliquen O., to be published in *Annu. Rev. Fluid Mech.* (2007).
[5] Andreotti B. and Douady S., *Phys. Rev. E*, **63** (2001) 031305.
[6] Ristow G. H., Riguidel F. X. and Bideau D., *J. Phys. I*, **4** (1994) 1161.
[7] Dippel S., Batrouni G. G. and Wolf D. E., *Phys. Rev. E*, **54** (1996) 6845.
[8] Ancey C., Evesque P. and Coussot P., *J. Phys. I*, **6** (1996) 725.
[9] Quartier L., Andreotti B., Douady S. and Daerr A., *Phys. Rev. E*, **62** (2000) 8299.
[10] Pouliquen O., *Phys. Fluids*, **11** (1999) 542; 1956.
[11] Johnson P. C., Nott P. and Jackson R., *J. Fluid Mech.*, **210** (1990) 501.
[12] Deboeuf S., Lajeunesse E., Dauchot O. and Andreotti B., *Phys. Rev. Lett.*, **97** (2006) 158303.